Journal of Engineering Mathematics **28**: 379–400, 1994.

Microwave heating of materials with impurities

T.R. MARCHANT

Department of Mathematics, University of Wollongong, Northfields Ave., Wollongong NSW 2522, Australia

Received 21 July 1992; accepted in revised form 9 November 1993

Abstract. The microwave heating of materials is important in many industrial processes. For example, it is used for the smelting of metals and the sintering of ceramics. Hot-spots (localised areas of high temperature) can develop in the material being heated or in the microwave oven itself, with disastrous consequences. Impurities in the material or in a component of the microwave oven can have different electromagnetic and thermal properties to the surrounding material. Different rates of heating occur at these sites, which gives rise to differential heating, which can lead to the generation of hot-spots. The generation of hot-spots by this mechanism is considered for a finite one-dimensional slab with a single impurity at its centre. A fixed-temperature boundary condition is applied at both ends of the slab and one end of the slab is irradiated by microwaves of constant amplitude. The heat absorption at the impurity is assumed to have a power-law dependence on temperature (hence hot-spot generation can occur via thermal runaway). Depending on the electrical and thermal properties of the material there are two possibilities; either a hot-spot occurs or a steady-state solution occurs due to a balance between heat absorption in the material and heat loss through the boundaries. These steady-state solutions are found for both linear and non-linear thermal absorptivity and constant and decaying electric-field amplitude. If possible the region of parameter space in which they occur (in the rest of the parameter space hot-spots occur) is also found. In addition, numerical solutions are developed to verify the steady-state solutions and to investigate cases where analytical solutions are difficult to derive, such as for materials with multiple impurities.

1. Introduction

There is presently considerable interest in the use of microwave radiation for heating in industrial processes such as drying, smelting, sintering, melting and sterilizing. The equations governing the microwave heating of a material can be shown to consist of the damped wave equation which governs the propagation of microwave radiation through the material and the forced heat equation which governs the resultant heat generation and flow. The forcing term in the heat equation is proportional to the square of the amplitude of the microwave field (Metaxas and Meredith [1]). In general, the properties of the material, such as electrical conductivity, electrical permittivity, magnetic permeability and thermal absorptivity are all temperature dependent, so that the equations are non-linearly coupled and therefore difficult to solve analytically. One phenomenon which is of particular interest is the generation of hot-spots, which results from temperature-dependent material properties. A hot-spot is a region which is much hotter than its surrounding, this phenomenon being both beneficial (smelting of metals) or harmful (baking of ceramics) to industrial microwave processes.

There have been two main approaches in the mathematical study of microwave heating. If the electromagnetic effects are of interest it is usually assumed that the material properties vary slowly with temperature, so that a perturbation solution may be found for both the electric field and the temperature. Kriegsmann et al. [2], Kriegsmann [3], Pincombe and Smyth [4], Smyth [5] and Marchant and Pincombe [6] have all used this approach. Alternatively, if the thermal aspects are isolated, as is frequently done in the study of hot-spots, then the electric-field amplitude is assumed constant and the forced heat equation

$$T_t = \nu T_{xx} + \gamma(T)\,, \tag{1.1}$$

considered, where $\gamma(T)$ is the temperature dependent rate of microwave absorption by the material (the thermal absorptivity) and the constant electric-field amplitude is normalised to unity. Roussy et al. [7] numerically solve (1.1) for a cylindrical body with the thermal absorptivity dependent on a quadratic function of temperature,

$$\gamma = \gamma_0 + \gamma_1 T + \gamma_2 T^2\,, \tag{1.2}$$

and a convective heat-loss boundary condition. Brodwin et al. [8] found steady-state solutions of (1.1) with the thermal absorptivity exponentially dependent on temperature,

$$\gamma = \gamma_0\, e^{\gamma_1 T}\,, \tag{1.3}$$

with convective and radiative heat-loss boundary conditions. They found that the steady-state temperature as a function of incident microwave power is an S-shaped curve. Hence beyond a certain critical power, a stable high temperature solution exists, i.e. a hot-spot. Coleman [9] considered a power-law dependency of the form

$$\gamma = \gamma_0(1 + \gamma_1 T)^{\gamma_2}\,, \tag{1.4}$$

and found that thermal runaway (an infinite temperature in finite time) occurs if $\gamma_1 > 0$, $\gamma_2 > 1$ and there is no diffusion ($\nu = 0$). Hill and Smyth [10] considered (1.1) and (1.3) for planar, cylindrical and spherical geometries with a fixed-temperature boundary condition and found steady-state solutions. They assumed that in the regions of parameter space where steady-state solutions do not occur, the hot-spots occur (in fact thermal runaway occurs due to the exponential thermal absorptivity). Also, for some parameter values, two steady-state solutions exist, with the higher temperature profile unstable and the lower temperature profile stable. Smyth [11] extends Hill and Smyth [10] to include temperature-dependent thermal diffusivity and constant electrical conductivity (which causes exponential decay of the electric-field amplitude). Again, steady-state solutions occur and it is reported that large electrical conductivity can prevent the occurrence of hot-spots. Hill and Jennings [12] analyse the experimental data collected for various materials to find simple analytical forms for the variation of thermal absorptivity with temperature. They find that in general, the thermal absorptivity increases with temperature. However, the thermal absorptivity can also decrease with temperature over a limited temperature range. In particular, they found linear, quadratic and exponential dependencies are valid for many materials.

Experimentally, it is found that hot-spots not only occur randomly in a material, but at an interface or join. For example, a hot-spot can occur between two sections of a microwave oven or waveguide held together with glue. This occurs because the glue has a higher thermal absorptivity than its surrounds; consequently differential heating can result in the generation of a hot-spot. Another example is that of microwave joining of polymers. An adhesive is used at the site to be joined, which is then cured using microwave radiation. Hot-spots can then occur at the join site during the heating process as the thermal absorptivity of the adhesive is higher than that of the base polymer. In the present work, generation of hot-spots by the mechanism of an impurity with a higher thermal absorptivity than the surrounding material is examined. A thermal absorptivity of the form

$$\gamma = \gamma_0 + (\gamma_1 + \gamma_2 T^{\gamma_3})\delta(x)\,, \tag{1.5}$$

is assumed, where $\delta(x)$ is a Dirac-delta function. This represents a material of constant thermal absorptivity with an impurity at $x = 0$. At the impurity there is a source of additional temperature-dependent thermal absorptivity. As mentioned, Hill and Jennings [12] find that a power-law description for the thermal absorptivity is valid for many materials, in particular, linear and quadratic ($\gamma_3 = 1$ or $\gamma_3 = 2$) power-laws fit the experimental data well. Here, only materials with thermal absorptivity increasing with temperature are considered, hence all the coefficients (γ_0, γ_1, γ_2 and γ_3) in (1.5) are positive.

A finite one-dimensional slab is considered with an impurity of the form (1.5) at its centre. At both ends of the slab a fixed-temperature boundary condition is applied. In a certain region of parameter space steady-state solutions occur as the heat absorption is balanced by heat loss through the boundaries; outside this region of parameter space hot-spots will occur. The electric-field amplitude (the heat absorption is proportional to the square of the amplitude) decays as the microwave radiation propagates through the slab, as a balance exists between energy lost from the electric field and the heat absorbed by the material. Hence, as the heat absorption is temperature dependent, so is the electric-field amplitude. In Sections 3 and 4 the electric-field amplitude is assumed constant (see Roussy et al. [7], Brodwin et al. [8], Coleman [9] and Hill and Smyth [10] for other microwave heating problems where this assumption is used). While this assumption is valid for very short slabs only (as the decay of the electric-field amplitude is small) it leads to a simple model of heat absorption and diffusion which allows hot-spot generation to be examined. In Section 3 linear thermal absorptivity is considered ($\gamma_3 = 1$). A long-time asymptotic solution is derived, using the Laplace transform, which shows steady-state, linearly-increasing and exponentially-increasing solutions. In Section 4 materials with non-linear thermal absorptivity are considered with steady-state solutions found. The temperature at the impurity is the solution of a transcendental equation, which is solved to obtain explicit steady-state solutions and conditions for hot-spot generation for some special choices of γ_3. In the appendix the explicit solutions of the transcendental equation obtained in Section 4 are found graphically. Also, in the appendix are additional explicit steady-state solutions, of more complicated form, along with a condition for hot-spot generation for arbitrary γ_3. In Section 5 steady-state solutions are found for nonlinear thermal absorptivity and decaying electric-field amplitude. As the electric-field amplitude depends on the temperature these solutions incorporate the interaction between the electric-field amplitude and the temperature. In Section 6 a numerical scheme is developed which is used to verify the analytical solutions. Also, a numerical solution is presented for a case for which an analytical solution is not easily derived, a slab with multiple impurities.

2. Governing equations

The equations governing the propagation of microwave radiation in a dielectric material are Maxwell's equations. In the case where the electrical permittivity ϵ, the magnetic permeability μ and the electrical conductivity σ are all slowly-varying functions of temperature, Maxwell's equations reduce to a damped wave equation of the form

$$E_{tt} + \sigma(T)E_t = c^2(T)E_{xx}\,, \tag{2.1}$$

(see Pincombe and Smyth [4]). As the microwave radiation propagates through the material,

it is damped due to the conductivity σ. Assuming that all the energy lost by the microwave radiation is converted into heat, the absorption and diffusion of heat in the material is governed by the forced heat equation

$$T_t = \nu T_{xx} + \gamma(x, T)|E|^2 , \tag{2.2}$$

where $|E|$ is the amplitude of the electric field, γ is the temperature-dependent thermal absorptivity and ν is the thermal diffusivity. A one-dimensional slab of finite length ($x \in [-1, 1]$) is considered with initial and boundary conditions

$$E(-1, t) = e^{-i\omega t} , \qquad E(x, 0) = T(\pm 1, t) = T(x, 0) = 0 , \tag{2.3}$$

The boundary conditions indicate that microwave radiation of constant amplitude unity and frequency ω is incident upon the boundary $x = -1$. A fixed-temperature boundary condition is applied at the ends of the slab (with the temperature normalised to zero). Initially, there is no electric field present in the material and the temperature is the constant ambient value (which is normalised to zero). It is assumed that the electric field is fully transmitted at both material boundaries with no reflection. The fixed-temperature boundary condition (2.3) applies in the large Biot-number limit. The Biot-number measures the relative effects of heat convection or radiation to heat diffusion. Hence, the fixed-temperature boundary condition (2.3) applies if the heat loss from the slab is significant with the slab's boundaries quickly cooled to the ambient temperature.

It is not possible to find an analytic solution to (2.1) and (2.2) with boundary and initial conditions (2.3) for general electrical conductivity, wavespeed and thermal absorptivity. By assuming particular forms for the material properties and that the frequency of the incident radiation is large, however, it is possible to find an analytic expression for the electric-field amplitude, which reduces the problem to that of finding a solution to the forced heat equation (2.2) subject to appropriate initial and boundary conditions.

It is assumed that the wavespeed is constant and that the thermal absorptivity is given by (1.5). This represents a base material with constant thermal absorptivity and an impurity at $x = 0$, where there is a source of additional temperature-dependent thermal absorptivity. For constant wavespeed, the thermal absorptivity must be proportional to the electrical conductivity so a balance is achieved between energy loss from the microwave radiation and heat absorption by the material. Hence, the electrical conductivity is

$$\sigma = \alpha(\gamma_0 + (\gamma_1 + \gamma_2 T^{\gamma_3})\delta(x)) , \tag{2.4}$$

where α is a constant of proportionality. To enable an expression for the electric-field amplitude to be derived the frequency of the microwave radiation is assumed large and a geometric optics expansion is performed (see Marchant and Pincombe [6] or Smyth [5]). The form

$$E = \phi(x, t)\, e^{i\omega\theta} + O(\omega^{-1}) , \quad \omega \gg 1 , \tag{2.5}$$

is assumed for the electric field, where the phase function θ represents the fast oscillations of the wavetrain while the amplitude ϕ is modulated by slow variations only. Expansion (2.5) is substituted into (2.1) and expanded in powers of ω. The transport equation

$$\phi_t + c\phi_x = -\frac{\sigma\phi}{2} , \tag{2.6}$$

results at $O(\omega)$ in the expansion. Equation (2.6) governs the evolution of the leading order amplitude ϕ. Solving (2.6) with electrical conductivity (2.4) by the method of characteristics gives

$$\phi = \exp\left[-\frac{\alpha}{2}(\gamma_0(x+1)+gu(x)\right]u(ct-x-1) \quad \text{where} \quad g=\gamma_1+\gamma_2 T^{\gamma_3}(0,t-x/c)\,, \tag{2.7}$$

as the leading order electric-field amplitude (u is the unit step function and α is a constant). Initially, the electric-field amplitude in the slab is zero; as the characteristic speed is c it takes time $t=2/c$ for the whole slab to be irradiated by the microwave radiation. As the characteristic speed is large ($c \gg 1$), this transient effect can be ignored as the timescale over which it occurs is much shorter than the timescale over which heat diffusion and absorption occurs. Assuming $c \gg 1$ in (2.7) gives

$$\phi = \exp\left[-\frac{\alpha}{2}(\gamma_0(x+1)+gu(x))\right] \quad \text{where} \quad g=\gamma_1+\gamma_2 T^{\gamma_3}(0,t)\,, \tag{2.8}$$

as the electric-field amplitude. If no impurity is present in the material (hence $g=0$) the electric-field amplitude decays exponentially with decay rate $\alpha\gamma_0/2$. With the impurity present, the solution in the region between the incident boundary (at $x=-1$) and the impurity (at $x=0$) is the same as if the electrical conductivity was constant (as the characteristic speed, c, is positive the impurity cannot affect the electric-field amplitude in the region $x<0$). At the impurity the electric-field amplitude is discontinuous; the electric field amplitude is reduced by a factor of $e^{-\alpha g/2}$ due to the temperature-dependent electrical conductivity located there. Hence, the electric-field amplitude is reduced in the region $x>0$ as the temperature increases. In the region $x>0$ the electric-field amplitude continues to decay exponentially with decay rate $\alpha\gamma_0/2$. With the form (2.8) for the electric-field amplitude the forced heat equation (2.2) becomes

$$T_t = T_{xx} + \gamma(x,T)\,e^{-\alpha(\gamma_0(x+1)+gu(x))}\,, \tag{2.9}$$

where γ is given by (1.5), g by (2.8) and the thermal diffusivity is normalised to unity. Hence, the total rate of heat absorption in the slab (the forcing term in (2.9)) is dependent on both the thermal absorptivity, which increases with temperature, and the electric-field amplitude, which decreases with temperature in the region $x>0$ (in the region $x<0$ it is independent of temperature).

An alternative formulation for (2.9) is to consider the relevant forced heat equation either side of the impurity

$$T_t = T_{xx} + \gamma_0\,e^{-\alpha\gamma_0(x+1)}\,, \quad x<0\,, \qquad T_t = T_{xx} + \gamma_0\,e^{-\alpha(\gamma_0(x+1)+g)}\,, \quad x>0\,, \tag{2.10}$$

supplemented by a jump condition, which is the integral of (2.9) over the impurity

$$T_x(x=0^+) - T_x(x=0^-) = -\frac{g}{2}e^{-\alpha\gamma_0}(1+e^{-\alpha g})\,, \quad \text{where} \quad g=\gamma_1+\gamma_2 T^{\gamma_3}(x=0)\,, \tag{2.11}$$

where the electric-field amplitude at the impurity is taken as the average of the amplitudes either side of the impurity. The appropriate initial and boundary conditions are

$$T(x,0) = T(\pm 1,t) = 0\,. \tag{2.12}$$

3. Long-time asymptotic solutions for linear thermal absorptivity

In this section it is assumed that the slab is thin, or that the electric conductivity is small so that the variation of the electric-field amplitude over the slab can be ignored (hence $\alpha = 0$). In addition the thermal absorptivity is assumed to vary linearly with temperature (hence $\gamma_3 = 1$). These two assumptions enable a simple model equation involving heat absorption and diffusion to be obtained, which enables some basic features of microwave heating and hot-spot generation to be illustrated. In particular, the model shows that over a certain parameter range a balance occurs between heat absorption in the material and heat loss through the boundaries, leading to a steady-state solution. Outside this parameter range hot-spots occur.

With the electric-field amplitude constant both of (2.10) are the same, hence the temperature profile is symmetric. Hence, the forced heat equation

$$T_t = T_{xx} + \gamma_0 , \tag{3.1}$$

needs to be considered only in the domain $x \in [0, 1]$. (3.1) is subject to initial and boundary conditions

$$2T(0, t)_x + \gamma_2 T(0, t) = \gamma_1 , \qquad T(1, t) = T(x, 0) = 0 . \tag{3.2}$$

The first of (3.2) represents the heat flow into the slab from the impurity while the second of (3.2) states that the temperature at the boundary is constant and the initial temperature is uniform (both normalised to zero). The solution to (3.1) and (3.2) can be found as an infinite series using the Laplace-transform or Fourier-series method. For example, Haberman [13, Section 5.8] derives details of a related problem using the Fourier-series methods. Here the Laplace-transform method is used to derive the solution. The Laplace transform is defined by

$$\bar{T}(x, s) = \int_0^\infty \mathrm{e}^{-st} T(x, t)\, \mathrm{d}t , \tag{3.3}$$

and after the transformation (3.1) becomes

$$\bar{T}_{xx} - s\bar{T} = -\frac{\gamma_0}{s} ,$$

subject to

$$2\bar{T}_x(0) + \gamma_2 \bar{T}(0) = -\frac{\gamma_1}{s} , \qquad \bar{T}(1) = 0 . \tag{3.4}$$

The solution to (3.4) is

$$\bar{T} = \frac{\gamma_1 \sinh\sqrt{s}(1 - |x|)}{sD(s)} + \frac{\gamma_0}{s^2}(1 - \cosh\sqrt{s}(1 - |x|)) + \frac{\gamma_0(2\sqrt{s}\sinh\sqrt{s} + \gamma_2(1 - \cosh\sqrt{s}))}{s^2 D(s)} \sinh\sqrt{s}(1 - |x|) ,$$

where

$$D(s) = 2\sqrt{s}\cosh\sqrt{s} - \gamma_2 \sinh\sqrt{s}\,. \tag{3.5}$$

Solution (3.5) is valid over the whole slab $x \in [-1, 1]$. It appears as though (3.5) diverges as $s \to \infty$, however writing $\bar{T}$ in terms of exponentials gives

$$\bar{T} = \frac{\gamma_0(s\gamma_1 + \gamma_2 - (2\sqrt{s} + \gamma_2)\,\mathrm{e}^{-\sqrt{s}})\,\mathrm{e}^{\sqrt{s}(1-|x|)}}{s^2((2\sqrt{s} - \gamma_2)\,\mathrm{e}^{\sqrt{s}} + (2\sqrt{s} + \gamma_2)\,\mathrm{e}^{-\sqrt{s}})} - \frac{\gamma_0(s\gamma_1 + \gamma_2 + (2\sqrt{s} - \gamma_2)\,\mathrm{e}^{\sqrt{s}})\,\mathrm{e}^{-\sqrt{s}(1-|x|)}}{s^2((2\sqrt{s} - \gamma_2)\,\mathrm{e}^{\sqrt{s}} + (2\sqrt{s} + \gamma_2)\,\mathrm{e}^{-\sqrt{s}})} + \frac{\gamma_0}{s^2}\,. \tag{3.6}$$

It can now be seen that $\bar{T} \to 0$ as $s \to \infty$ (which implies $T = 0$ at time $t = 0$ as required). The form (3.5) is used to find the long-term behaviour though, due to its simpler form. The solution to (3.1) and (3.2) is obtained using the transformed solution $\bar{T}$ derived above. The inverse Laplace transform is given by

$$T = \frac{1}{2\pi i}\int_{a-i\infty}^{a+i\infty} \bar{T}\,\mathrm{e}^{st}\,\mathrm{d}s\,, \tag{3.7}$$

where a must be chosen so that the path of integration is to the right of any singularities. The integral can be performed directly by summing the residues of the poles of $\bar{T}$. The solution is found as an infinite series; each term in the series is the residue of a pole with the residues being calculated in descending order in size of the real part of the pole. The residues of the poles with the largest real parts (the real part of the pole represents the exponential growth or decay rate in the solution) represent the most important contributions to the solution at long times, hence the first terms of the series represents an approximation to the solution at long times. For $\gamma_2 = 0$ all the terms of the infinite series are found, while for $\gamma_2 \neq 0$ only the first term of the series is found to get an approximation valid for a long time.

(a) $\gamma_2 = 0$

The transform (3.5) with $\gamma_2 = 0$ is

$$\bar{T} = \left(\frac{\gamma_1}{2s^{3/2}} + \frac{\gamma_0}{s^2}\sinh\sqrt{s}\right)\frac{\sinh\sqrt{s}(1-|x|)}{\prod_{n=0}^{\infty}\left(1 + \dfrac{4s\pi^2}{(2n+1)^2}\right)} + \frac{\gamma_0}{s^2}(1 - \cosh\sqrt{s}(1-|x|))\,, \tag{3.8}$$

where the product form of $\cosh\sqrt{s}$ has been used to write $\bar{T}$ in terms of its poles. All the poles of (3.8) are real with the largest at $s = 0$ and the rest of the poles negative. Hence, the simple pole at $s = 0$ represents steady terms while the other poles represent exponentially decaying terms. Summing the residues of the poles of (3.8) gives

$$\begin{aligned} T = {} & \left(\frac{\gamma_1}{2} + \gamma_0\right)(1-|x|) - \frac{\gamma_0}{2}(1-|x|)^2 \\ & + \frac{1}{\pi^3}\sum_{n=0}^{\infty}\left(\frac{\gamma_1}{2}\frac{(-1)^{n+1}}{(n+\frac{1}{2})^4\pi} - \frac{2\gamma_0}{(n+\frac{1}{2})^3}\right)\sin((n+\tfrac{1}{2})\pi(1-|x|))\,\mathrm{e}^{-(n+1/2)^2\pi^2 t}\,, \end{aligned} \tag{3.9}$$

which represents a steady-state solution plus an infinite sum of transients. The temperature evolves to a steady-state parabolic profile as the heat absorbed by the material is balanced by heat loss through the boundaries.

(b) $\gamma_2 > 0$

In this case $D(s)$, the denominator of (3.5), cannot be exactly written as a product of its

zeros (which are all real). The largest zero of $D(s)$ is considered to enable an approximation valid at long times to be derived. Three qualitatively different solutions exist depending on the value of γ_2.

(i) $0 < \gamma_2 < 2$

In this case $D(s)$ has no positive zeros, so all the poles of (3.5) are either zero or negative. Let $D(s) = \sqrt{s}F(s)$ where $F(s)$ only has negative zeros (so it represents the transient decay terms). The transform (3.5) becomes

$$\bar{T} = \frac{\gamma_1}{s^{3/2}} \frac{\sinh\sqrt{s}(1-|x|)}{F(s)} + \frac{\gamma_0}{s^{5/2}} \frac{(2\sqrt{s}\sinh\sqrt{s} + \gamma_2(1-\cosh\sqrt{s}))\sinh\sqrt{s}(1-|x|)}{F(s)}$$
$$+ \frac{\gamma_1}{s^2}(1-\cosh\sqrt{s}(1-|x|)\,. \tag{3.10}$$

The residue of the simple pole at $s = 0$ gives

$$T = \frac{(2\gamma_1 + 4\gamma_0 - \gamma_2\gamma_0)}{2(2-\gamma_2)}(1-|x|) - \frac{\gamma_0}{2}(1-|x|)^2 + 0(e^{-\alpha t})\,, \tag{3.11}$$

where α is the decay rate of the largest transient. The temperature evolves towards a steady-state parabolic profile as in the case of $\gamma_2 = 0$. Figure 1 shows the temperature T versus x for $\gamma = 0.1 + (0.3 + 0.3T)\delta(x)$ and $t = 10$. Compared are (3.11) and the numerical solution (6.2) (——). There is an excellent comparison between the curves. There is a maximum in the temperature profile at $x = 0$ as there is less heat loss from the centre of the slab than from near the boundaries and as there is more heat being absorbed at the impurity. The heat absorption is balanced by heat loss through the boundaries, so a steady-state solution results.

(ii) $\gamma_2 > 2$

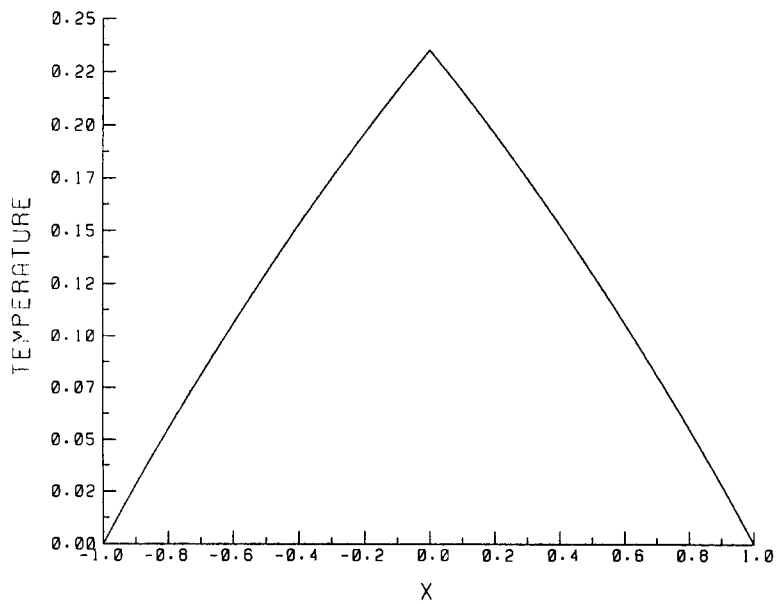

Fig. 1. Temperature T versus x for $\gamma = 0.1 + (0.3 + 0.3T)\delta(x)$, $t = 10$ and a fixed temperature boundary condition. Compared are the asymptotic theory (3.11) and the numerical solution (6.2) (——).

In this case $D(s)$ has one positive zero; hence (3.5) has one positive pole. Let $D(s) = (s - r_1)F(s)$ where r_1 is the positive zero and $F(s)$ has only non-positive zeros which represent the transients. So (3.5) becomes

$$\bar{T} = \frac{\gamma_1}{s}\frac{\sinh\sqrt{s}(1-|x|)}{(s-r_1)F(s)} + \frac{\gamma_0}{s^2}\frac{(2\sqrt{s}\sinh\sqrt{s} + \gamma_2(1-\cosh\sqrt{s}))\sinh\sqrt{s}(1-|x|)}{(s-r_1)F(s)} + \frac{\gamma_0}{s^2}(1-\cosh\sqrt{s}(1-|x|)) . \tag{3.12}$$

Summing the residues of the simple pole at $s = r_1$ gives

$$T = \frac{\gamma_1 + \frac{\gamma_0}{r_1}(2r_1^{1/2}\sinh r_1^{1/2} + \gamma_2(1-\cosh r_1^{1/2}))}{\left(1-\frac{\gamma_2}{2}\right)\cosh r_1^{1/2} - r_1^{1/2}\sinh r_1^{1/2}}\sinh r_1^{1/2}(1-|x|)\,e^{r_1 t} + O(1) . \tag{3.13}$$

Here the heat absorbed by the material cannot be balanced by heat loss at the boundaries and consequently the dominant term in (3.13) increases exponentially. The zero r_1 can be found by solving for the zeros of $D(s)$ numerically (by Newton's method for example).

(iii) $\gamma_2 = 2$

In this case $D(s)$ has no positive zeros, so the poles of (3.5) are either zero or negative. Let $D(s) = s^{3/2}F(s)$ where $F(s)$ has only negative zeros. The transform (3.5) becomes

$$\bar{T} = \frac{\gamma_1}{s^{5/2}}\frac{\sinh\sqrt{s}(1-|x|)}{F(s)} + \frac{\gamma_0}{s^2}(1-\cosh\sqrt{s}(1-|x|)) + \frac{\gamma_0}{s^{7/2}}\frac{(2\sqrt{s}\sinh\sqrt{s} + \gamma_2(1-\cosh\sqrt{s}))}{F(s)}\sinh\sqrt{s}(1-|x|) . \tag{3.14}$$

Summing the residue of the double pole at $s = 0$ gives

$$T = \frac{3}{2}t(\gamma_0 + \gamma_1)(1-|x|) + O(1) . \tag{3.15}$$

In this case the dominant term represents a triangular temperature profile which increases linearly with time.

In summary, the rate of change of heat absorption with temperature, γ_2, is the parameter which determines the qualitative form of the solution. For $\gamma_2 < 2$ a balance between heat absorption by the material and heat loss through the boundaries occurs and a steady-state solution results, while for $\gamma_2 \geq 2$ a hot-spot results. For $\gamma_2 > 2$ the temperature increases exponentially with time, while $\gamma_2 = 2$ is a transition case where a linear increase in temperature with time occurs.

4. Steady-state solutions for non-linear thermal absorptivity

4.1. The general solution and its stability

In Section 3 long-time asymptotic solutions are developed for a finite-one dimensional slab with an impurity which has linear thermal absorptivity and constant electric-field amplitude.

Here, non-linear thermal absorptivity of the form (1.5) is considered with the electric-field amplitude again constant. Thus, the heat absorption and diffusion are described by (2.8) with the electrical-field amplitude constant ($\alpha = 0$). As in Section 3 the temperature profile is symmetric, hence the forced heat equation (3.1) is considered on the domain $x \in [0, 1]$ subject to the initial and boundary conditions

$$2T_x(0, t) + \gamma_2 T^{\gamma_3}(0, t) = -\gamma_1 , \qquad T(1, t) = T(x, 0) = 0 . \tag{4.1}$$

In general, (4.1) is non-linear (except for $\gamma_3 = 0$, $\gamma_2 = 0$ or $\gamma_3 = 1$) so the Laplace-transform method of Section 3 is inapplicable. Section 3 showed that for a fixed-temperature boundary condition, steady-state solutions are possible as the heat absorption in the material is balanced by the heat loss through the boundaries (for $\gamma_3 = 1$ steady-state solutions occur for $\gamma_2 < 2$). To find steady-state solutions of (3.1), take $T_t = 0$, integrate and apply the fixed-temperature boundary condition (the second of (4.1)), which gives

$$T = a_1 - \left(a_1 - \frac{\gamma_0}{2}\right)|x| - \frac{\gamma_0}{2}x^2 , \tag{4.2}$$

where a_1 is a constant. Note that the solution is valid over the whole slab ($x \in [-1, 1]$). Applying the first of (4.1) gives a_1, the temperature at the impurity, as the solution to the transcendental equation

$$\gamma_2 a_1^{\gamma_3} - 2a_1 + \gamma_0 + \gamma_1 = 0 . \tag{4.3}$$

A steady-state solution exists if (4.3) has a real positive zero (as a_1 is the temperature at the impurity it must be real and positive).

To investigate the stability of the steady-state solution (4.2) and (4.3), a linear stability analysis similar to Hill and Smyth [10] is performed. Let $T_s(x)$ be the steady-state solution (4.2) and look for perturbed solutions of the form

$$T(x, t) = T_s(x) + \epsilon u(x)\, e^{\lambda t} , \tag{4.4}$$

where ϵ is a small parameter, λ is the growth or decay rate of the perturbation and $u(x)$ is to be determined. At $O(\epsilon)$

$$u_{xx} - \lambda u = -u\gamma_3\gamma_2 T_s^{\gamma_3 - 1}\delta(x) , \quad u(\pm 1) = 0 , \tag{4.5}$$

is obtained, with the solution being

$$u = A\sqrt{\lambda}\,\sinh\sqrt{\lambda}(1 - |x|) , \tag{4.6}$$

where A is a constant and λ must satisfy the equation

$$\sqrt{\lambda} = \frac{\gamma_3\gamma_2 a_1^{\gamma_3 - 1}}{2}\tanh\sqrt{\lambda} . \tag{4.7}$$

For the temperature profile $T_s(x)$ to be stable (4.7) must have no positive solutions. Hence, the stability condition can be shown to be

$$\gamma_3\gamma_2 a_1^{\gamma_3 - 1} < 2 . \tag{4.8}$$

4.2. Some special cases

In general, (4.3) needs to be solved numerically; however explicit solutions can be found in some cases. Presented here are explicit solutions for the cases $\gamma_3 = 1/2$, $\gamma_3 = 1$ and $\gamma_3 = 2$. In particular, $\gamma_3 = 1$ and $\gamma_3 = 2$ are physically valid choices for many materials, see Hill and Jennings [12]. These solutions illustrate the qualitative nature of the solution in the various parameter regimes. In the appendix the explicit solutions to (4.3) presented here are found graphically in order to gain some insight into the nature of the solutions. Also, additional explicit solutions to (4.3) for the special cases $\gamma_3 = 1/4$, $\gamma_3 = 1/3$, $\gamma_3 = 3$ and $\gamma_3 = 4$ are presented in the appendix, due to their more complicated forms.

(a) $\gamma_3 = \frac{1}{2}$

In this case (4.3) has one positive real solution

$$a_1^{1/2} = \frac{\gamma_2 + \sqrt{\gamma_2^2 + 8(\gamma_0 + \gamma_1)}}{4}. \tag{4.9}$$

The steady-state temperature profile ((4.2) with a_1 given by (4.9)) is stable for all parameter values. Hence, in this case, heat absorption in the material is always balanced by heat loss through the boundaries.

(b) $\gamma_3 = 1$

In this case, (4.3) has one real positive solution $a_1 = (\gamma_0 + \gamma_1)/(2 - \gamma_2)$ if $\gamma_2 < 2$ and none otherwise. The steady-state temperature profile ((4.2) with a_1 given above) is the same as the long-time limit of (3.11). The stability condition (4.8) becomes $\gamma_2 < 2$, which confirms the stability result obtained in Section 3. Hence, for $\gamma_2 < 2$ heat absorption in the material is always balanced by heat loss through the boundaries, while for $\gamma_2 \geq 2$ a balance is not possible, hence a hot-spot occurs.

(c) $\gamma_3 = 2$

In this case (4.3) has the two real positive solutions

$$a_1 = \frac{1 \pm \sqrt{1 - \gamma_2(\gamma_0 + \gamma_1)}}{\gamma_2}, \tag{4.10}$$

if

$$\gamma_2(\gamma_0 + \gamma_1) < 1. \tag{4.11}$$

The stability condition (4.8) indicates that of the two steady-state temperature profiles ((4.2) with a_1 given by (4.10)), the profile of higher temperature is unstable while the profile of lower temperature is stable. The limiting steady-state temperature profile, below which all the stable steady-state temperature profiles lie, occurs when the two steady-state temperature profiles coalesce ($\gamma_2(\gamma_0 + \gamma_1) = 1$). No steady-state temperature profiles exist if the parameters lie outside the region (4.11) (so hot-spots occur). Figure 2 shows the two steady-state temperature profiles (4.2) (with a_1 given by (4.11)) and thermal absorptivity $\gamma = 0.5 + (0.5 + 0.95T^2)\delta(x)$ and the numerical solution (6.2) (——). The comparison between the lower (stable) temperature profile and the numerical solution is excellent. The higher temperature profile is unstable. Hill and Smyth [10] also find a similar pattern with their two temperature profiles, the one of higher temperature being unstable, while the one of lower temperature being stable.

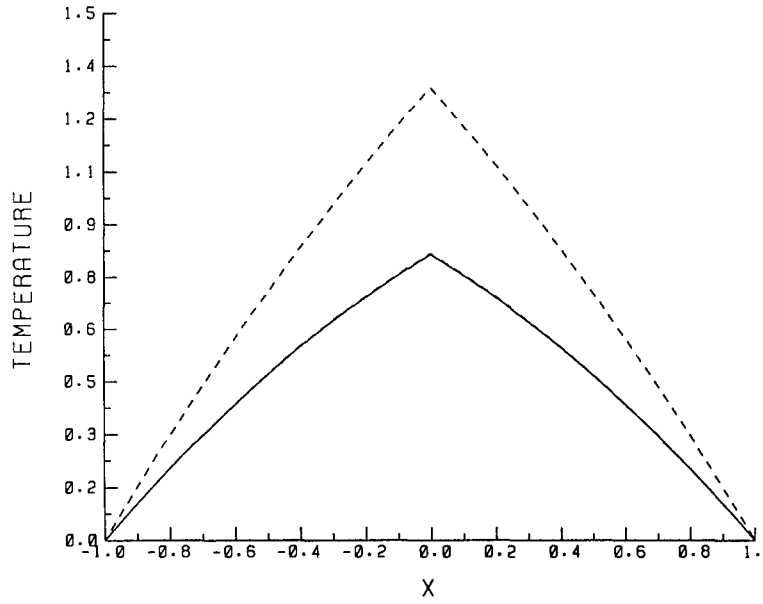

Fig. 2. Temperature T versus x for $\gamma = 0.5 + (0.5 + 0.95T^2)\delta(x)$. Compared are the two steady-state temperature profiles ((4.2) with (4.11)) and the numerical solution (6.2) (——).

In the appendix, stability conditions (the region of parameter space for which stable steady-state solutions exist) are derived explicitly for the special cases $\gamma_3 = 3$ and 4. In addition, a stability condition for arbitrary $\gamma_3 > 1$ is found. For $\gamma_3 > 1$, steady-state solutions occur in the region of parameter space (A.11) while outside this region hot-spots result (thermal runaway occurs). For $\gamma_3 < 1$, the stability condition (4.8) is always satisfied (which can be easily shown by rearranging (4.3)), hence only steady-state solutions occur and hot-spots are not possible. For $\gamma_3 = 1$ the results of Section 3 show that steady-state solutions occur for $\gamma_2 < 2$ while for $\gamma_2 \geq 2$ hot-spots occur (linearly-increasing solutions and exponentially-increasing solutions are both possible).

5. Steady-state solutions with a decaying electric-field amplitude

In Sections 3 and 4 steady-state solutions have been obtained by considering simple models of heat absorption and diffusion whilst ignoring the decay of the electric-field amplitude. Smyth [11] and Hill and Pincombe [14] both include the effect of decaying electric-field amplitude in their models by assuming the electrical conductivity is constant (hence the electric-field amplitude undergoes exponential decay as it propagates from the incident boundary). Here the form (2.8) is used for the electric-field amplitude thus including both the decay of the electric-field amplitude as it propagates from the incident boundary and the interaction of the amplitude with the temperature in the model.

The forced heat equation (2.10) is considered subject to the jump condition (2.11) and initial and boundary conditions (2.12). To find steady-state solutions take $T_t = 0$, integrate, apply the jump condition (2.11) and the initial and boundary conditions (2.12) to obtain

$$T = \frac{1}{\alpha^2\gamma_0}(1 - e^{-\alpha\gamma_0(x+1)}) + c_1(x+1), \quad x<0$$
$$T = \frac{e^{-\alpha(g+\gamma_0)}}{\alpha^2\gamma_0}(e^{-\alpha\gamma_0} - e^{-\alpha\gamma_0 x}) + c_2(x-1), \quad x>0, \tag{5.1}$$

where the constants c_1 and c_2 are given by

$$c_1 = \frac{1}{2\alpha^2\gamma_0}(e^{-\alpha\gamma_0}-1)(e^{-\alpha(g+\gamma_0)}+1) - \frac{e^{-\alpha\gamma_0}}{2\alpha}(1-e^{-\alpha g}) + \frac{g}{4}e^{-\alpha\gamma_0}(1+e^{-\alpha g}),$$
$$c_2 = \frac{1}{2\alpha^2\gamma_0}(e^{-\alpha\gamma_0}-1)(e^{-\alpha(g+\gamma_0)}+1) + \frac{e^{-\alpha\gamma_0}}{2\alpha}(1-e^{-\alpha g}) - \frac{g}{4}e^{-\alpha\gamma_0}(1+e^{-\alpha g}), \tag{5.2}$$

and $g = \gamma_1 + \gamma_2 a_1^{\gamma_3}$. The temperature at the impurity, a_1, is the solution to the transcendental equation

$$\frac{1}{\alpha^2\gamma_0}(1-e^{-\alpha\gamma_0}) + \frac{1}{2\alpha^2\gamma_0}(e^{-\alpha\gamma_0}-1)(e^{-\alpha(g+\gamma_0)}+1) - \frac{e^{-\alpha\gamma_0}}{2\alpha}(1-e^{-\alpha g})$$
$$+ \frac{g}{4}e^{-\alpha\gamma_0}(1+e^{-\alpha g}) = a_1. \tag{5.3}$$

In the limit $\alpha \to 0$ (where there is a no decay of the electric-field amplitude) (5.1) and (5.2) become the solution (4.2) and (4.3) as required. The temperature profile (5.1) is not symmetric like the temperature profiles found in Sections 3 and 4. This is because the electric-field amplitude decays exponentially (in addition the amplitude is reduced by a factor of $e^{-\alpha g}$ at the impurity) away from the incident boundary $x = -1$. Hence, less heat is absorbed in the region $x>0$ than in the region $x<0$ resulting in a non-symmetric temperature profile. By performing a stability analysis similar to that in Section 4.1 the stability condition for the profile (5.1) is found to be

$$\gamma_3\gamma_2 a_1^{\gamma_2-1} e^{-\alpha\gamma_0}(1+e^{-\alpha g}) < 4, \tag{5.4}$$

with a_1 given by (5.3). In the limit $\alpha \to 0$ (5.4) becomes the stability condition (4.8) as required.

For the case of $\gamma_3 = 1$ an explicit stability condition can be found, as in Section 4. In this case, as the temperature profile becomes marginally stable the temperature becomes large ($a_1 \to \infty$). Hence, let $e^{-\alpha g} = 0$ in (5.3) to obtain

$$a_1 = \frac{2 - 2(1+\alpha\gamma_0)e^{-\alpha\gamma_0} + \alpha^2\gamma_0\gamma_1 e^{-\alpha\gamma_0}}{\alpha^2\gamma_0(4-\gamma_2 e^{-\alpha\gamma_0})}, \quad \gamma_2 \to 4e^{\alpha\gamma_0}, \tag{5.5}$$

as the temperature at the impurity. Hence the temperature profile is positive and stable if

$$\gamma_2 < 4e^{\alpha\gamma_0}. \tag{5.6}$$

As α increases the bound on γ_2 such that a stable steady-state temperature profile exists also increases; this is because large α corresponds to a large decay in the electric-field amplitude, which in turn leads to less heat absorption. In the limit $\alpha \to 0$ (5.6) the bound for stable steady-state solutions ($\gamma_2 < 4$) is different from that found for materials with linear thermal

absorptivity and constant electric-field amplitude (cf. $\gamma_2 < 2$ from Section 4). The limits are different because the limiting stable temperature profile ((5.5) in the limit $\gamma_2 \to 4\,e^{\alpha\gamma_0}$) becomes unbounded (hence $a_1 \to \infty$). This means $e^{-\alpha g} \to 0$ for any finite α whereas in Section 4 it is assumed that $\alpha = 0$ (hence $e^{-\alpha g} = 1$). Physically, in Section 4 it is assumed that the electric-field amplitude is constant throughout the slab, while here, in the limit $\alpha \to 0$, the electric-field amplitude is constant in the region $x < 0$ and zero in the region $x > 0$ (due to the large temperature at the impurity). Hence, the bound on γ_2 is twice as large as that found in Section 4.

Figure 3 shows stable steady-state temperature profiles (5.1) for thermal absorptivity $\gamma = 5 + (2 + 1.8T)\delta(x)$ with $\alpha = 0.05$, 0.1, 0.2 and 0.4. The case $\alpha = 0$ (not shown) corresponds to zero electrical conductivity (hence there is no decay of the electric-field amplitude) and the temperature profile is symmetric with a maximum temperature $T = 35$ at the impurity. As α increases the decay of the electric-field amplitude is increased, hence the heat absorption is less, which in turn lowers the steady-state temperature profiles. In addition, the temperature profiles become less nearly symmetric as α increases and if the decay of the electric-field amplitude is high enough the temperature peak occurs before the impurity (see the $\alpha = 0.4$ curve).

Figure 4 shows the temperature T versus x for $\alpha = 1.5$, $\gamma = 1 + (1 + 0.6T^2)\delta(x)$ and $t = 10$. Shown is the numerical solution (6.2) (——) and the steady-state temperature profile (5.1). There is an excellent comparison between the curves. Because the conductivity is large ($\alpha = 1.5$) the temperature profile is unsymmetric with the temperature higher in the region $x < 0$ than in the region $x > 0$ (due to the decay of the electric-field amplitude from the boundary at $x = -1$). The temperature profile in the region $x > 0$ is approximately linear; as almost no heat absorption occurs there (the electric-field amplitude is very small in this region; it is effectively damped by the high temperature at the impurity), all the heating occurs via heat diffusion from the impurity at $x = 0$. For this choice of thermal absorptivity,

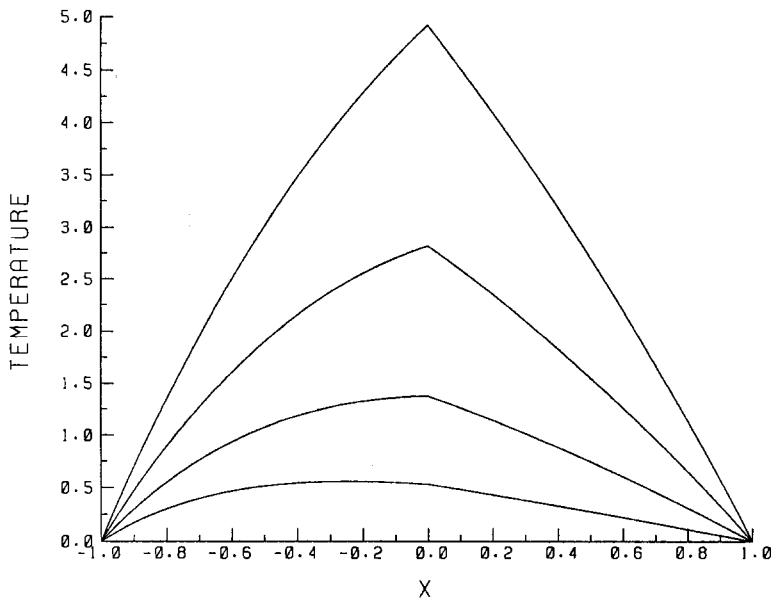

Fig. 3. Temperature T versus x for $\gamma = 5 + (2 + 1.8T)\delta(x)$ and $\alpha = 0.05$, 0.1, 0.2 and 0.4. Shown are the steady-state temperature profiles (5.1).

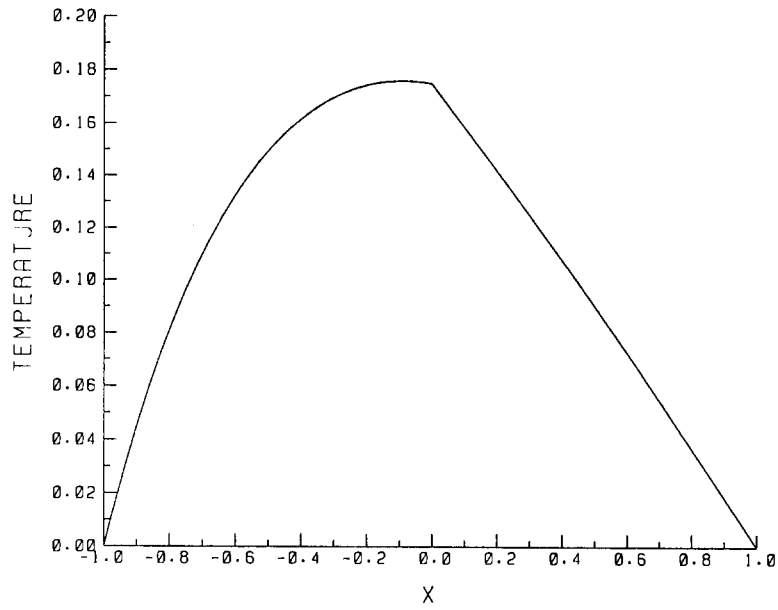

Fig. 4. Temperature T versus x for $\alpha = 1.5$, $t = 10$ and $\gamma = 1 + (1 + 0.6T^2)\delta(x)$. Compared are the steady-state temperature profile (5.1) and the numerical solution (6.2) (——).

γ, thermal runaway would occur if the electric-field amplitude was constant (as $\gamma_2(\gamma_0 + \gamma_1) = 1.2 > 1$). With $\alpha = 1.5$ however, a steady-state temperature profile occurs due to the lowered heat absorption. This confirms the results of Smyth [11] who reports that non-zero electrical conductivity can stop hot-spots from occurring.

6. Numerical solutions

In order to verify the accuracy of the steady-state solutions derived in the previous sections and to model situations for which analytical solutions are difficult to derive (such as a slab with multiple impurities) a numerical scheme for the forced heat equation (2.10) subject to the jump condition (2.11) and the initial and boundary conditions (2.12) is developed. The solution at time t is

$$T(p, q) = T(-1 + p\,\Delta x, q\,\Delta t)\,, \quad p = 0, 1, \ldots, n\,, \tag{6.1}$$

where $q = t/\Delta t$, and $n = 2/\Delta x$. The scheme for calculating the solution at time $t = (q + 1)\,\Delta t$ is

$$-\frac{s}{2}T(p+1, q+1) + (1+s)T(p, q+1) - \frac{s}{2}T(p-1, q+1)$$
$$= \frac{s}{2}T(p+1, q) + (1-s)T(p, q) + \frac{s}{2}T(p-1, q) + \gamma_0\,\mathrm{e}^{-\alpha\gamma_0 p\,\Delta x}\,\Delta t\,, \quad p = 1, \ldots, \frac{n}{2} - 1\,,$$
$$T\left(\frac{n}{2} - 1, q+1\right) - 2T\left(\frac{n}{2}, q+1\right) + T\left(\frac{n}{2} + 1, q+1\right) = -\frac{g(q)}{2}\,\mathrm{e}^{-\alpha\gamma_0}(1 + \mathrm{e}^{-\alpha g(q)})\,\Delta x\,,$$
$$-\frac{s}{2}T(p+1, q+1) + (1+s)T(p, q+1) - \frac{s}{2}T(p-1, q+1)$$

$$= \frac{s}{2} T(p+1, q) + (1-s)T(p, q) + \frac{s}{2} T(p-1, q) + \gamma_0 \, e^{-\alpha(\gamma_0 + g(q))p \, \Delta x} \, \Delta t \,,$$

$$p = \frac{n}{2} + 1, \ldots, n-1 \,, \qquad s = \frac{v \, \Delta t}{(\Delta x)^2} \quad \text{and} \quad g(q) = \gamma_1 + \gamma_2 T^{\gamma_3}\left(\frac{n}{2}, q\right). \tag{6.2}$$

The first and third of (6.2) is the discretisation of (2.10) in the regions $x<0$ and $x>0$, respectively. The finite-difference scheme used is the Crank–Nicolson scheme, which is unconditionally stable for the unforced heat equation ((6.2) with $\gamma = 0$) and no numerical evidence of instability has been found for the forced equation. The second of (6.2) is the discretisation of the jump condition (2.11) which is applied at the impurity ($x = 0$). The initial and boundary conditions are

$$T(j, 0) = T(0, j) = T(n, j) = 0 \,, \quad \forall j \,, \tag{6.3}$$

which state that initially the slab is of zero temperature and that the temperature at both boundaries is fixed at zero.

Figure 5 shows the temperature T versus x for $\alpha = 0.1$, $\gamma = 0.1 + (1 + 3T^2)(\delta(x + 1/3) + \delta(x - 1/3))$ and $t = 0.7$. This represents a finite slab with two impurities, one at $x = -1/3$ the other at $x = 1/3$. Temperature peaks occur at both of the impurities. The temperature at $x = 1/3$ is less than the temperature at $x = -1/3$ due to decay of the electric-field amplitude in the slab (which results from the non-zero temperature-dependent electrical conductivity). As time increases, the temperature peak at the impurity located at $x = 1/3$ fades as the temperature rises at the impurity located at $x = -1/3$ (where thermal runaway occurs). This is because the initial hot-spot reduces the electric-field amplitude in the region $x > -1/3$. Hence, thermal runaway occurs at the impurity closest to the boundary at which the microwaves are incident; it damps out the microwave radiation in the rest of the slab.

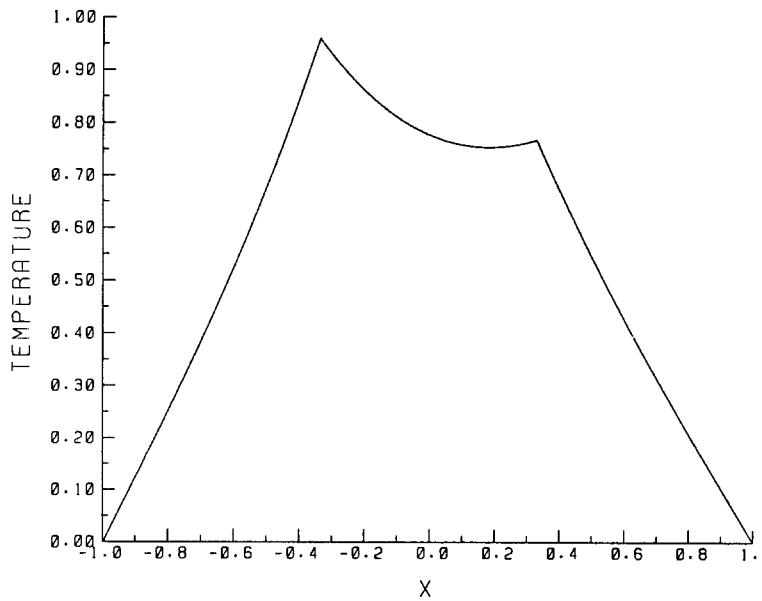

Fig. 5. Temperature T versus x for $\alpha = 0.1$, $t = 0.7$ and $\gamma = 0.1 + (1 + 3T^2)(\delta(x + 1/3) + \delta(x - 1/3))$. Shown is the numerical solution (6.2).

7. Conclusion

The microwave heating of a finite one-dimensional slab is considered with an impurity located at its centre. This impurity has temperature-dependent thermal absorptivity, hence a hot-spot can occur in the slab (due to thermal runaway). As cooling occurs at the boundaries (a fixed-temperature boundary condition is applied) a steady-state temperature profile is also possible, dependent on the specific values of the material properties. Steady-state solutions are found for linear and non-linear thermal absorptivity and for constant and decaying electric-field amplitude. The region of parameter space in which stable steady-state solutions occur (in the rest of the parameter space hot-spots occur) are also found for some special cases.

When the dependency on temperature of the heat absorption is less than linear ($\gamma_3 < 1$) then a hot-spot can never occur as there will always be a balance between heat absorption and heat loss through the boundaries leading to a steady-state solution. For ($\gamma_3 \geqslant 1$) both hot-spots and steady-state solutions are possible, depending on the other parameter values. The parameter regions in which table steady-state solutions occur are given explicitly for linear, quadratic, cubic and quartic dependencies (see Section 4 and the appendix). In addition, a stability condition for arbitrary $\gamma_3 > 1$ is found. Decaying electric-field amplitude decreases (but does not eliminate) the possibility of hot-spots, due to less heat being absorbed in the material.

This study shows that in real applications of microwave technology it is important to know how the dielectric properties of the material being heated vary with temperature. Once these properties have been found experimentally (normally the electrical permittivity and the loss tangent are tabulated, see Von Hippel [15]) then the functional form of the thermal absorptivity, γ, can be found (see Hill and Jennings [12]). This then allows the results of Sections 4 and 5 (after suitable scalings) to determine if a hot-spot is likely to occur.

Extensions to this work could involve the study of two- and three-dimensional bodies and the use of cylindrical and spherical co-ordinates to investigate the microwave heating of more realistic material geometries such as plates, rods and pellets. In addition, materials with temperature-dependent properties throughout, rather than just at the impurity could be considered; of particular interest would be the interaction of the temperature with the electric-field amplitude in this case.

Appendix

In Section 4 steady-state solutions are obtained for a material with non-linear thermal absorptivity and constant electric-field amplitude throughout. The temperature at the impurity is found by solving for the real positive roots of the transcendental equation $y(x) = 0$ where

$$y(x) = \gamma_2 x^{\gamma_3} - 2x + \gamma_0 + \gamma_1 \,. \tag{A.1}$$

In this appendix, the explicit solutions of (A.1), found in Section 4.2 for the special cases $\gamma_3 = 1/2$, $\gamma_3 = 1$ and $\gamma_3 = 2$ are found graphically in order to gain some additional insight into the nature of the solutions. Additional explicit solutions to (A.1), for the special cases $\gamma_3 = 1/4$, $\gamma_3 = 1/3$, $\gamma_3 = 3$ and $\gamma_3 = 4$ are also presented. Lastly, the graphical method used above is generalised to obtain the stability condition for arbitrary $\gamma_3 > 1$.

1. The graphical solutions

In Section 4.2 the temperature at the impurity is found by solving (A.1) for the special cases $\gamma_3 = 1/2$, $\gamma_3 = 1$ and $\gamma_3 = 2$. Here, (A.1) is solved graphically for these special cases, in order to gain some insight into the nature of the solutions. Figure 6 shows $y(x)$ versus x for $\gamma_3 = 1/2$ and $\gamma_0 = \gamma_1 = 1$. The curves are drawn for $\gamma_2 = 0.01$, 0.5 and 1. Also shown is $y = 0$ (– – –). Hence, the intersection of the solid and dashed lines represents the solutions of (A.1) (given by (4.9) for $\gamma_3 = 1/2$). For $\gamma_2 = 0.01$ the curve is approximately a straight line with the root occurring at $x \approx 1$. As γ_2 increases the root increases in magnitude. It can be seen that the y-intercept is always positive (as $\gamma_0 + \gamma_1 > 0$) and $y \to -\infty$ as $x \to \infty$ (as the term $-2x$ dominates $\gamma_2 x^{1/2}$ in this limit), hence there exists a real positive root of (A.1) for all parameter values (it is easy to show that $y' < 0$ for all x greater than the root, hence there is only one real positive root). This is in agreement with Section 4.2(a) where the explicit solution to (A.1) for $\gamma_3 = 1/2$ is presented.

Figure 7 shows $y(x)$ versus x for $\gamma_3 = 2$ and $\gamma_0 = \gamma_1 = 1$. The curves are drawn for $\gamma_2 = 0.4$, 0.5 and 0.6. Also shown is $y = 0$ (– – –). Hence, the intersection of the solid and dashed lines represents the solutions of (A.1) (given by (4.10) for $\gamma_3 = 2$). For $\gamma_2 = 0.4$ there are two real positive roots, while for $\gamma_2 = 0.5$ these coalesce into one real positive root. As γ_2 is increased further the parabolic curve is shifted in the positive y-direction with the result being no positive real roots exist for the case $\gamma_2 = 0.6$. This is in agreement with Section 4.2(c) where the explicit solutions to (A.1) for $\gamma_3 = 2$ are presented. By examining Fig. 7, the parameter values for which the two real positive roots coalesce (and hence the stability condition) for a material with a quadratic thermal absorptivity can be found. Take both

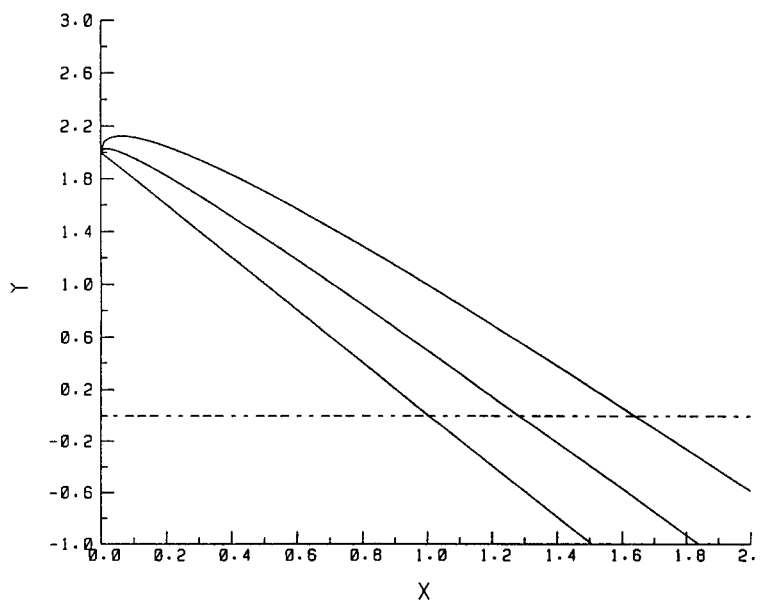

Fig. 6. $y(x)$ versus x for $\gamma_3 = 1/2$ and $\gamma_0 = \gamma_1 = 1$. The curves are drawn for $\gamma_2 = 0.01$, 0.5 and 1. Also shown is $y = 0$ (– – –).

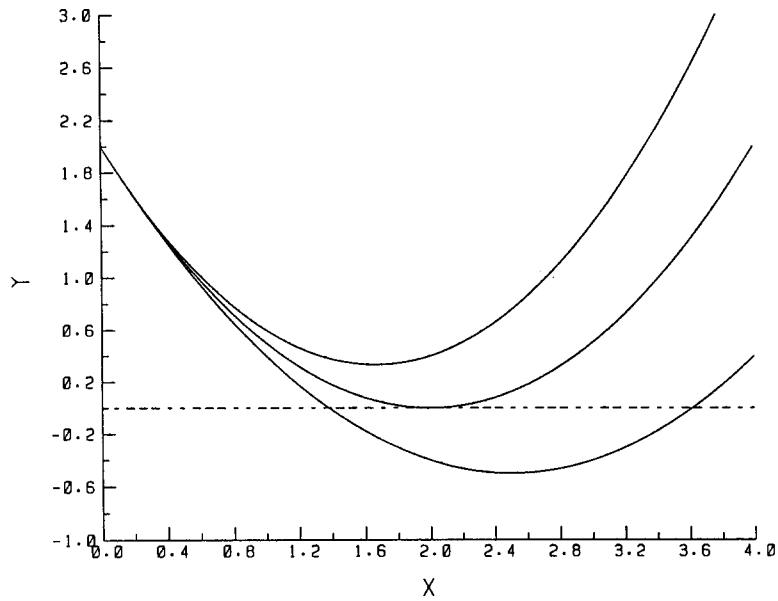

Fig. 7. $y(x)$ versus x for $\gamma_3 = 2$ and $\gamma_0 = \gamma_1 = 1$. The curves are drawn for $\gamma_2 = 0.4$, 0.5 and 0.6. Also shown is $y = 0$ (---).

$$\begin{aligned} y(x) &= \gamma_2 x^2 - 2x + \gamma_0 + \gamma_1 = 0\,, \\ y'(x) &= 2\gamma_2 x - 2 = 0\,, \end{aligned} \tag{A.2}$$

which simply state that the transcendental equation and its derivative are zero for the case where the two roots coalesce (hence the root occurs at the turning point of the transcendental equation). Solving (A.2) gives the relation

$$\gamma_2(\gamma_0 + \gamma_1) = 1\,, \tag{A.3}$$

which is precisely the relationship given by (4.10) for one real positive root to occur. In Fig. 7 the roots coalesce in the case $\gamma_2(\gamma_0 + \gamma_1) = 0.5(1 + 1) = 1$ which satisfies (A.3). As the temperature profile is unstable in this case (see (4.8)) the inequality corresponding to (A.3) (see (4.11)) gives the stability condition for the heating of a material with a quadratic thermal absorptivity.

For the case of linear thermal absorptivity ($\gamma_3 = 1$) the qualitative nature of the solution is easily explained without the aid of a figure. The γ-intercept of (A.1) is positive, hence for a real positive root to exist, the slope of the line, $\gamma_2 - 2$, must be negative. This is true if $\gamma_2 < 2$ which is precisely the stability condition obtained in Section 4.2(b).

2. *Additional explicit solutions*

Here the explicit solutions obtained in Section 4.2 are supplemented by explicit solutions to (4.3) for the special cases $\gamma_3 = 1/4$, $\gamma_3 = 1/3$, $\gamma_3 = 3$ and $\gamma_3 = 4$.

(a) $\gamma_3 = \frac{1}{4}$
In this case (4.3) has one positive real solution,

$$a_1^{1/4} = \frac{u_1^{1/2}}{2} + \frac{(2(u_1^2 + 2(\gamma_0 + \gamma_1))^{1/2} - u_1)^{1/2}}{2}, \tag{A.4}$$

where $u_1 = (q + d^{1/2})^{1/3} + (q - d^{1/2})^{1/3}$.

and $q = \gamma_2^2/8$, $p = -2(\gamma_0 + \gamma_1)/3$ and $d = q^2 - p^3$.

(b) $\gamma_3 = \frac{1}{3}$
In this case (4.3) has one positive real solution,

$$a_1^{1/3} = (q + d^{1/2})^{1/3} + (q - d^{1/2})^{1/3}, \quad \text{for } d \geqslant 0,$$
$$a_1^{1/3} = 2\left(\frac{\gamma_2}{6}\right)^{1/2} \cos(\phi), \quad \text{where } \cos(3\phi) = qp^{-3/2}, \quad \text{for } d < 0. \tag{A.5}$$

and $p = \gamma_2/6$, $q = (\gamma_0 + \gamma_1)/4$ and $d = q^2 - p^3$.

(c) $\gamma_3 = 3$
In this case there are two real positive solutions

$$a_1 = 2\left(\frac{2}{3\gamma_2}\right)^{1/2} \cos(\phi), \qquad a_1 = -2\left(\frac{2}{3\gamma_2}\right)^{1/2} \cos(\phi + \pi/3), \tag{A.6}$$

where $\cos(3\phi) = -\left(\frac{\gamma_0 + \gamma_1}{2\gamma_2}\right)\left(\frac{3\gamma_2}{2}\right)^{3/2}$,

if $\gamma_2(\gamma_0 + \gamma_1)^2 < 32/27$. (A.7)

(d) $\gamma_3 = 4$
In this case there are two real positive solutions

$$a_1 = \frac{u_1^{1/2}}{2} \pm \frac{\left(2\left(u_1^2 - 4\left(\frac{\gamma_0 + \gamma_1}{\gamma_2}\right)\right)^{1/2} - u_1\right)^{1/2}}{2}, \tag{A.8}$$

where $u_1 = (q + d^{1/2})^{1/3} + (q - d^{1/2})^{1/3}$,

if $\gamma_2(\gamma_0 + \gamma_1)^3 < 27/16$. (A.9)

The other parameters in (A.8) and (A.9) are given by $q = 2/\gamma_2^2$, $3p = 4(\gamma_0 + \gamma_1)/\gamma_2$ and $d = q^2 - p^3$. In cases (a) and (b) where $\gamma_3 = 1/4$ and $\gamma_3 = 1/3$, respectively, the steady-state solutions are qualitatively similar to the case $\gamma_3 = 1/2$. There is one steady-state solution which is stable for all parameter values. Hence, heat absorption is always balanced by heat loss through the boundaries. In cases (c) and (d) where $\gamma_3 = 3$ and $\gamma_3 = 4$, respectively, the steady-state solutions are qualitatively similar to the case $\gamma_3 = 2$. There are two steady-state solutions; the lower temperature profile is stable ((4.2) with a_1 given by the second of (A.6) and (A.8), respectively) while the higher temperature profile is unstable ((4.2) with a_1 given by the first of (A.6) and (A.8), respectively). In the case where the two steady-state temperature profiles coalesce ($\gamma_2(\gamma_0 + \gamma_1)^2 = 32/27$ and $\gamma_2(\gamma_0 + \gamma_1)^3 = 27/16$, respectively) the limiting steady-state temperature profile is unstable. There are no steady-state solutions outside the regions of parameter space (A.7) and (A.9) (hence hot-spots occur).

3. The stability condition for arbitrary γ_3

The method for finding when the two real positive zeros of (A.1) coalesce for quadratic thermal absorptivity (and thus the stability condition) can be generalised to all $\gamma_3 > 1$. Consider (A.1) and its derivative

$$y'(x) = \gamma_3\gamma_2 x^{\gamma_3 - 1} - 2 = 0\,. \tag{A.10}$$

Note the correspondence between (A.10) and the stability condition (4.8). Solving (A.1) and (A.10) gives the stability condition

$$\gamma_2(\gamma_0 + \gamma_1)^{\gamma_3 - 1} < \left(\frac{2}{\gamma_3}\right)^{\gamma_3} (\gamma_3 - 1)^{\gamma_3 - 1}\,, \quad \gamma_3 > 1. \tag{A.11}$$

The temperature at the impurity for the limiting temperature profile (which occurs when the two steady-state solutions coalesce) is given by

$$a_1 = \left(\frac{2}{\gamma_2\gamma_3}\right)^{1/(\gamma_3 - 1)}\,, \quad \gamma_3 > 1\,. \tag{A.12}$$

Note that for $\gamma_3 < 1$ there is no limiting temperature profile as a stable steady-state solution exists for all parameter values (the explanation of Fig. 6 proves that one steady-state solution always exists while stability is easily shown by rearranging (4.3)). Substituting $\gamma_3 = 2$, 3, and 4 into (A.11) gives the stability conditions (4.11), (A.7) and (A.9), respectively, as required. While substituting $\gamma_3 = 2$, 3, and 4 into (A.12) gives the appropriate expressions for the temperature at the impurity for the limiting temperature profile (see (4.10), (A.6) and (A.8), respectively).

As γ_3 becomes large ($\gamma_3 \to \infty$), the temperature at the impurity for the limiting temperature profile $a_1 \to (\gamma_0 + \gamma_1)/2$. As $\gamma_3 \to \infty$ the heat absorbed due to the temperature-dependent thermal absorptivity at the impurity for this limiting temperature profile increases if $\gamma_0 + \gamma_1 \geqslant 2$. This is because the temperature at the impurity is greater than unity. Hence the bound on γ_2, given by (A.11), for a stable steady-state solution to exist decreases to zero as $\gamma_3 \to \infty$. Conversely, as $\gamma_3 \to \infty$ the heat absorbed due to the temperature-dependent thermal absorptivity at the impurity for the limiting temperature profile decreases if $\gamma_0 + \gamma_1 < 2$. This is because the temperature at the impurity is less than unity. Hence, the bound on γ_2, given by (A.11), for a stable steady-state solution to exist increases without limit as $\gamma_3 \to \infty$.

Acknowledgement

The author wishes to thank one of the referees for some very useful suggestions.

References

1. A.S. Metaxas and R.J. Meredith, *Industrial Microwave Heating*. IEE Power Engineering Series, 4, P. Peregrinus on behalf of the Institution of Electrical Engineers, London (1983).
2. G.A. Kriegsmann, M.E. Brodwin and D.G. Watters, Microwave heating of a ceramic halfspace. *SIAM J. Appl. Math.* 50 (1990) 1088–1098.

3. G.A. Kriegsmann, Thermal runaway in microwave heated ceramics: a one-dimensional model. *J. Appl. Phys.* 71 (1992) 1960–1966.
4. A.H. Pincombe and N.F. Smyth, Microwave heating of materials with low conductivity. *Proc. Roy. Soc. Lond.* A 433 (1991) 479–498.
5. N.F. Smyth, Microwave heating of bodies with temperature dependent properties. *Wave Motion* 12 (1990) 171–186.
6. T.R. Marchant and A.H. Pincombe, Microwave heating of materials with temperature dependent wavespeed. *Wave Motion* (1994) to appear.
7. G. Roussy, A. Bennani and J. Thiebaut, Temperature runaway of microwave irradiated materials. *J. Appl. Phys.* 62 (1987) 1167–1170.
8. M.E. Brodwin, G.A. Kriegsmann and D.G. Watters, Temperature instability in the microwave heating of a uniformly illuminated planar slab. *IEEE* (1994) to appear.
9. C.J. Coleman, On the microwave hotspot problem. *J. Aust. Math. Soc.* B 33 (1991) 171–186.
10. J.M. Hill and N.F. Smyth, On the mathematical analysis of hotspots arising from microwave heating. *Math. Eng. in Industry* 2 (1990) 267–278.
11. N.F. Smyth, The effect of conductivity on hot-spots. *J. Austral. Math. Soc.* B 33 (1992) 403–413.
12. J.M. Hill and M.J. Jennings, Formulation of model equations for heating by microwave radiation. *Appl. Math. Modelling* 17 (1993) 1823–1834.
13. R. Haberman, *Elementary Applied Partial Differential Equations*. Prentice-Hall, New Jersey (1983).
14. J.M. Hill and A.H. Pincombe, Some similarity profiles for the microwave heating of a half-space. *J. Austral. Math. Soc. Ser.* B 33 (1991) 290–320.
15. A.R. Von Hippel, *Dielectric Materials and Applications*. MIT Press, Cambridge, MA (1954).